dine (50%, 20 ml) was added and the mixture was extracted with *n*-pentane. The solution was filtered to remove the urea, rendered anhydrous after 18 hr, and evaporated with pyridine. The residue was dissolved in a mixture of dry pyridine (2.5 ml) and acetic acid (2.5 ml). The solution was heated at 40° for 5 hr and precipitated with ether and *n*-pentane (3:2). The precipitate was collected by centrifugation and washed with ether. It was treated with DCC (310 mg) in pyridine (10 ml) and triethylamine (0.7 ml, 0.088 mmol) for 2 days at room temperature. Water (10 ml) was added and the solution was extracted with *n*-pentane (10 ml, 3 portions). The solution was filtered and diluted with 95% ethyl alcohol (20 ml) and applied to a column of TEAE-cellulose (acetate). The elution pattern and conditions are shown in Figure 3. The trinucleotide VII was eluted in peak IV. Fractions of 561–610 were combined and evaporated with pyridine. The residual syrup was dissolved in water (200 ml) and extracted with *n*-butyl alcohol (100 ml and 50 ml, 3 portions). *n*-Butyl alcohol was evaporated and the product was precipitated from its pyridine solution with ether and *n*-pentane (3:2). The yield was 1060 OD_{260} units, 17%.

Pyridinium 5′-O-Monomethoxytrityl-N,2′-O-dibenzoylcytidylyl-(3′–5′)-N,2′-O-diacetylguanylyl-(3′–5′)-uridine 3′-Phosphate. The cyclic phosphate VII was treated with pancreatic RNase (2.5 mg) in a mixture of DMF (1.5 ml), 1 *M* ammonium acetate (1 ml), and water (7.5 ml) at 37° for 9 hr. Paper chromatography and electrophoresis at this stage showed a small amount of the starting material and the incubation was further continued with addition of the enzyme (1 mg) for 8 hr. The reaction mixture was passed through a column (1.2 × 10 cm) of pyridinium Dowex 50X2. The column was washed with a mixture of pyridine (5 ml), ethyl alcohol (50 ml), DMF (20 ml), and water (25 ml). The effluent and washings were used for the next step.

Pyridinium 5′-O-Monomethoxytrityl-N,2′-O-dibenzoylcytidylyl-(3′–5′)-N-2′,O-diacetylguanylyl-(3′–5′)-2′-O-acetyluridine 3′-Phosphate (VIII). The trinucleotide from the above experiment was added to tetraethylammonium acetate (6 mmol) and evaporated with added pyridine five times. The residue was coevaporated with toluene four times to remove pyridine and treated with acetic anhydride (0.57 ml, 6 mmol) for 3 days at room temperature. The reaction mixture was cooled in an ice bath and cooled 50% aqueous pyridine (200 ml) was added. The solution was passed through a column (1.2 × 25 cm) of pyridinium Dowex 50X2 and the column was washed with 50% pyridine. The effluent and washings were evaporated with pyridine and the anhydrous pyridine solution was added to a mixture of ether and *n*-pentane (3:2, v/v) with vigorous stirring. The precipitate was collected by centrifugation and washed with the same mixture of ether and *n*-pentane. The purity of the trinucleotide was checked by paper chromatography. R_f values of the trinucleotide derivatives are shown in Table I. Acetic acid (80%) treatment and successive methanolic ammonia treatment gave the unprotected trinucleotide, CpGpUp, which was completely digested by RNase M to yield Gp (1.1 OD_{260} units), Up (0.96 OD_{260} unit), and Cp (1.28 OD_{280} units) in 0.05 *N* HCl after separation by paper chromatography (solvent C) and paper electrophoresis (pH 3.5).

Acknowledgment. The authors thank Dr. Masachika Irie of the University of Kyoto for his generous gift of RNase M, Kojin Co. Ltd. for ribonucleotides, and Dr. Marvin Caruthers for reading the manuscript. This work was partly supported by Matsunaga Science Foundation to which the authors' thanks are due.

π-Cation Radicals and Dications of Metalloporphyrins[1]

J. Fajer,[2a] D. C. Borg,[2b] A. Forman,[2b] D. Dolphin,[2c] and R. H. Felton[2d]

Contribution from the Department of Applied Science and the Medical Department, Brookhaven National Laboratory, Upton, New York 11973, the Department of Chemistry, Harvard University, Cambridge, Massachusetts 02138, and the Department of Chemistry, Georgia Institute of Technology, Atlanta, Georgia 30332. *Received October 24, 1969*

Abstract: Zinc tetraphenylporphyrin (ZnTPP) and magnesium octaethylporphyrin (MgOEP) undergo reversible one- and two-electron oxidations. Removal of the first electron by controlled potential electrolysis or by oxidation with xenon difluoride or bromine results in cation radicals whose esr spectra clearly indicate electron abstraction from the porphyrin ring. The observed hyperfine structure is assigned, with the help of deuterium labeling, to interaction of the unpaired electron with the *meso* protons of $MgOEP^+$ and with the protons on the *phenyl* groups of $ZnTPP^+$. Electronic absorption spectra of the radicals, dications, and of a dimer of $MgOEP^+$ which exists at low temperatures are presented. The results of an SCF–MO study are compared with the experimental esr and optical data. These calculations suggest that a radical may occupy either of two close-lying ground states. We conclude that the ground-state symmetries of $ZnTPP^+$ and $MgOEP^+$ are, respectively, $^2A_{2u}$ and $^2A_{1u}$ of the D_{4h} point group.

Crucial steps in photosynthetic and metabolic processes involve metalloporphyrin redox properties. Prior studies of heme function have stressed the redox characteristics of the central metal;[3,4] in contradistinction, primary photosynthetic events involving chlorophyll appear to depend upon ring redox properties.[5,6]

A striking feature of the porphyrin ring is its ability to undergo facile reduction and oxidation. Reductions of chlorophyll[7] and metalloporphyrins,[8] dissolved in aprotic solvents, have been accomplished by electrochemical and chemical techniques, and the results

(1) Aspects of this work were previously presented: (a) J. Fajer, D. C. Borg, D. Dolphin, and R. H. Felton, Abstracts, 157th National Meeting of the American Chemical Society, Minneapolis, Minn., April 1969, p 130; (b) R. H. Felton, D. Dolphin, D. C. Borg, and J. Fajer, *J. Amer. Chem. Soc.*, 91, 196 (1969).

(2) (a) Department of Applied Science, Brookhaven National Laboratory; (b) Medical Department, Brookhaven National Laboratory; (c) Harvard University; (d) Georgia Institute of Technology.

(3) J. E. Falk, "Porphyrins and Metalloporphyrins," Elsevier Publishing Co., New York, N. Y., 1964.

(4) B. Chance, R. W. Estabrook, and T. Yonetani, Ed., "Hemes and Hemoproteins," Academic Press, New York, N. Y., 1966.

(5) B. Kok, *Biochim. Biophys. Acta*, 48, 527 (1961).

(6) J. Weikard, A. Muller, and H. T. Witt, *Z. Naturforsch.*, 18b, 139 (1963).

(7) R. H. Felton, G. W. Sherman, and H. Linschitz, *Nature*, 203, 637 (1964).

(8) G. L. Closs and L. E. Closs, *J. Amer. Chem. Soc.*, 85, 818 (1963); N. Hush and J. Dodd, *J. Chem. Soc.*, 4607 (1964); D. Clack and N. Hush, *J. Amer. Chem. Soc.*, 87, 4238 (1965); R. H. Felton and H. Linschitz, *ibid.*, 88, 1113 (1966).

clearly demonstrate the formation of π-anion radicals and dianions. On the other hand, the oxidative sequence of metalloporphyrins is not as well established. Chlorophyll may be oxidized or photooxidized, but the resultant species has been variously formulated as a neutral free radical occurring *via* hydrogen atom loss,[9] a radical formed by nucleophillic attack on a cation radical,[10] or the cation radical itself.[9,11]

A similar, confused situation exists with porphyrins. Ceric ion oxidation of various metallophthalocyanins and free base tetraphenylporphyrin was reported to proceed through a one-electron intermediate, characterized as a π-electron cation.[12] Later polarographic studies in butyronitrile led Stanienda to propose that metalloporphyrins[13] and chlorophyll[14] could be oxidized by two successive, one-electron abstractions, and he formulated these as cations in which the positive charge is localized on the nitrogen atoms. Siderov, *et al.*, photolyzed zinc etioporphyrin I in frozen methylene chloride–chloroform solutions and obtained a species which was postulated to be a cation radical.[15]

Fuhrhop and Mauzerall demonstrated that magnesium[16a] as well as other metallooctaethylporphyrins[16b] can be chemically oxidized in a reversible one-electron step. They called attention to additional interactions which can affect the porphyrin cations such as ligand distortions, aggregation, complexing, and the specific role of the metal atom. Concurrently, we carried out electrochemical and chemical oxidations of octaethyl (OEP) and tetraphenylporphyrins (TPP). We found evidence[1] of two successive, reversible one-electron oxidations which yielded (a) π-cation radicals and dications (TPP and OEP complexes of Mg, Zn, Cd, Cu), (b) oxidized metals followed by π cations [CoTPP and CoOEP: $Co(II)P \rightarrow Co(III)P^{+} \rightarrow Co(III)P^{2+}$]. Cobalt(III) etioporphyrin had previously been reported.[17] Recently, Manassen and Wolberg,[18] after investigating a series of tetraphenylporphyrins, also concluded that removal of the electron may occur from the metal or the ligand.

The present paper continues our reports on the preparation, characterization, and electronic structure of oxidized metalloporphyrins. Additional experimental evidence is presented that ZnTPP and MgOEP form stable π-cation radicals and dications. Theoretical considerations suggest that nearly degenerate ground states of the oxidized species may result in quite diverse esr spectra for closely related compounds.

(9) H. Linschitz and J. Rennert, *Nature*, **169**, 193 (1952).
(10) B. Diehn and G. R. Seely, *Biochim. Biophys. Acta*, **153**, 862 (1968).
(11) E. I. Rabinowitch and J. Weiss, *Proc. Roy. Soc.* (London), **162A**, 251 (1937); W. F. Watson, *J. Amer. Chem. Soc.*, **75**, 2522 (1953); J. C. Goedheer, G. H. Horreus De Haas, and P. Schuller, *Biochim. Biophys. Acta*, 28, 61, 278 (1958).
(12) P. George, D. J. E. Ingram, and J. E. Bennett, *J. Amer. Chem. Soc.*, **79**, 1870 (1957).
(13) A. Stanienda and G. Biebl, *Z. Phys. Chem.* (Frankfurt am Main), **52**, 254 (1967).
(14) A. Stanienda, *Z. Phys. Chem.* (Leipzig), **229**, 257 (1965).
(15) A. N. Sidorov, V. Ye. Kholmogorov, R. P. Yestigneyeva, and G. N. Kol'tsova, *Biofizika*, **13**, 143 (1968).
(16) (a) J.-H. Fuhrhop and D. Mauzerall, *J. Amer. Chem. Soc.*, **90**, 3875 (1968); (b) J.-H. Fuhrhop and D. Mauzerall, *ibid.*, **91**, 4174 (1969).
(17) G. Engelsma, A. Yamamoto, E. Markham, and M. Calvin, *J. Phys. Chem.*, **66**, 2517 (1962).
(18) J. Manassen and A. Wolberg, Abstracts, 158th National Meeting of the American Chemical Society, New York, N. Y., Sept 1969, PHYS-028.

Experimental Section

Materials. Dichloromethane was distilled from CaH_2. It was collected and stored over molecular sieves (Linde, No. 5A or 3A). Chloroform was passed through a column of basic alumina (Woelm, grade 1). Methanol was distilled from magnesium turnings. Butyronitrile was stirred at room temperature with $KMnO_4$ and distilled at reduced pressure. This treatment was repeated twice followed by distillation from CaH_2. Toluene was distilled from molten sodium. These solvents were also degassed and stored *in vacuo* over the appropriate desiccant. Tetrapropylammonium perchlorate (TPAP) was prepared by neutralization of the corresponding hydroxide with $HClO_4$ followed by two recrystallizations from absolute ethanol. The compound was stored in a vacuum oven at 60° and vented to argon before use. Xenon difluoride was synthesized by exposure of a Pyrex bulb containing $^2/_3$ atm of fluorine and $^1/_3$ atm of xenon to sunlight. The product was isolated and purified by standard methods.[19] Argon was used directly or after passage through a titanium furnace operated at 550°. Bromine was used directly from freshly opened bottles.

Porphyrins. Benzaldehyde-d_5 was prepared by oxidation of benzene-d_6 with aluminum chloride and dichloromethyl methyl ether according to Rieche, *et al.*[20] Mass spectroscopic analysis showed >98% deuterium incorporation into the aromatic ring.

***meso*-Tetraphenyl-d_{20}-porphyrin** was synthesized by condensation of benzaldehyde-d_5 and pyrrole in acetic acid. The product was chromatographed on neutral alumina (Woelm, grade II) eluted with chloroform, and crystallized from chloroform–alcohol: $\lambda_{max}^{CH_2Cl_2}$ nm ($\epsilon \times 10^{-4}$) 417(47.2), 517(1.91), 551(1.00), 592(0.55), 651 (0.45); $\lambda_{max}^{CF_3CO_2H}$ ($\epsilon \times 10^{-4}$) 436(45.0), 653(4.55); mass spectra (70 eV) *m/e* (rel intensity) 637(4), 636(13), 635(46), 634(100), 633 (46), 632(20), 631(7), 630(2), 629(1), 628(<0.5); *m/e* 634.3717, $C_{44}H_{10}D_{20}N_4$ requires *m/e* 634.3705. (This corresponds to 96% deuterium in the phenyl rings.)

***meso*-Tetra(*o*-fluorophenyl)porphyrin** was similarly prepared in propionic acid from pyrrole and *o*-fluorobenzaldehyde and crystallized from dichloromethane–methanol: mp >300°; $\lambda_{max}^{CH_2Cl_2}$ nm ($\epsilon \times 10^{-3}$), 416(462), 511(21.9), 543(4.13), 587(6.67), 646(2.31); $\lambda_{max}^{CF_3CO_2H}$ nm ($\epsilon \times 10^{-3}$), 432(475), 584(11.0), 635(284); mass spectrum (70 eV) *m/e* (rel intensity) 689(5), 688(16), 687(51), 686(100), 685(6); *m/e* 686.2095, $C_{44}H_{26}F_4N_4$ requires *m/e* 686.2093. (The corresponding *meta* and *para* isomers as well as the pentafluoro derivative (H_2TPP-f_{20}) were all readily synthesized by condensation of pyrrole with the appropriate aldehyde in propionic acid.)

Zinc tetraphenylporphyrins (including the fluorine- and deuterium-substituted compounds) were prepared by heating the appropriate H_2TPP with zinc acetate and sodium acetate in acetic acid. The resulting zinc complexes were chromatographed on neutral alumina (Woelm or BioRad) with benzene and crystallized from dichloromethane–methanol.

Zinc *meso*-tetraphenyl-d_{20}-porphyrin showed the following characteristics: $\lambda_{max}^{CH_2Cl_2}$ nm ($\epsilon \times 10^{-4}$), 420(54.2), 584(2.0); mass spectrum (70 eV) *m/e* (rel intensity) 703(2), 702(4), 701(13), 700(34), 699(44), 698(72), 697(82), 696(100), 695(89), 694(52), 693(26), 692(12), 691(5), 690(3). This corresponds to 93% deuterium in the phenyl rings; *m/e* 696.2829, $C_{44}H_8D_{20}N_4Zn$ requires *m/e* 696.2840 (for Zn = 63.9291).

Zinc *meso*-tetra(*o*-fluorophenyl)porphyrin exhibited the following: $\lambda_{max}^{CH_2Cl_2}$ nm ($\epsilon \times 10^{-3}$), 415(612), 544(24.7); *m/e* 748.1217, $C_{44}H_{24}F_4N_4Zn$ requires *m/e* 748.1228.

***meso*-d_4-Octaethylporphyrin.**[21] Octaethylporphyrin was dissolved in D_2SO_4–D_2O (9:1) and allowed to stand for 3 hr. The solution was poured onto ice and the amorphous product filtered and washed with water. The porphyrin was dried over potassium carbonate in chloroform, isolated, and crystallized from dichloromethane–methanol: mass spectrum (70 eV), *m/e* (rel intensity) 485(2), 484(12), 483(48), 482(100), 481(12), 480(3), 479(2), 478(1). This corresponds to 93% incorporation of deuterium at the *meso* positions.

Magnesium *meso*-d_4-Octaethylporphyrin. *meso*-d_4-Octaethylporphyrin was suspended in dry benzene and methylmagnesium iodide in ether was added. The solution was stirred for 30 min followed by addition of D_2O. The porphyrin contained in the organic layer was dried over potassium carbonate, isolated, and recrystallized

(19) D. R. MacKenzie and J. Fajer, *Inorg. Chem.*, **5**, 699 (1966), and references therein.
(20) A. Rieche, H. Gross, and E. Hoft, *Chem. Ber.*, **93**, 88 (1960).
(21) R. Bonnett and G. S. Stephenson, *Proc. Chem. Soc.* (London), 291 (1964).

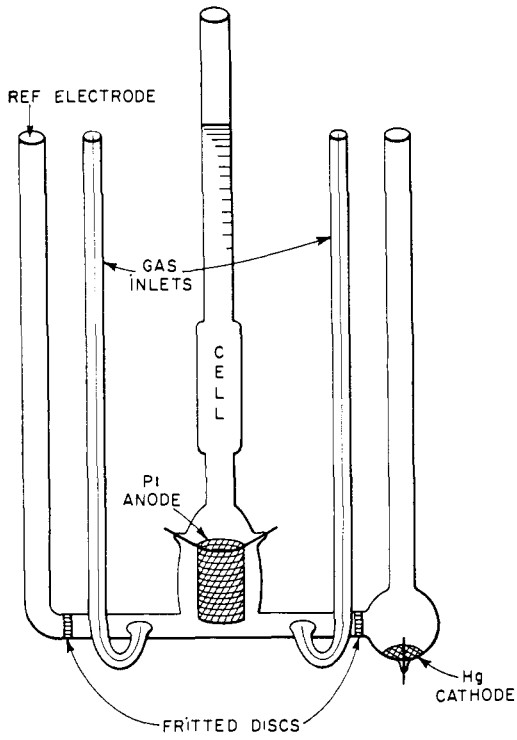

Figure 1. Controlled potential electrolysis cell used for optical measurements.

from nitromethane: $\lambda_{max}^{CH_2Cl_2}$ nm ($\epsilon \times 10^{-4}$), 410(38.0), 543(1.71), 580(1.57); mass spectrum (70 eV) *m/e* (rel intensity) 565(0.25), 564(1.5), 563(8), 562(29), 561(58), 560(100), 559(9), 558(1.5), 557 (0.5). This corresponds to d_4 (91%), d_3 (8%), d_2 (1.2%), d_1 (0.5%); *m/e* 560.3651, $C_{36}H_{40}D_4N_4Mg$ requires *m/e* 560.3663 (for Mg = 23.98504).

The porphyrins were stored overnight in a vacuum oven at 60°, vented to argon, pumped overnight at 10^{-6} Torr, and vented to argon to remove water or solvent of crystallization.

Electrolytic Oxidations. Bulk electrolyses were carried out at controlled potentials. The coulometric titrator, similar to ORNL Model Q-2005-X50, has been described by Kelley, *et al.*[22] Electrolysis was performed in a three-electrode cell while a selected potential was applied between the reference and the controlled electrodes. A known fraction of the current was electronically integrated; the number of coulombs passed during the electrolysis was obtained by measuring the voltage output of the integrator. The design of the cell used for controlled-potential electrolysis allowed *in situ* optical measurements. A platinum gauze basket (Figure 1) suspended below a quartz optical cell of 1.0-mm light path served as the controlled electrode. A fritted disk of medium porosity separated the anolyte from the mercury cathode while a coarse disk isolated the reference electrode compartment. Argon gas, introduced through the capillaries, stirred and deaerated the solution. Aqueous saturated calomel acted as the reference electrode through a potassium chloride–agar bridge; all potentials discussed in the text are referred to this electrode.

A typical run consisted of filling the compartments of the electrolysis cell (dried in a vacuum oven at 60° for 12 hr and vented to argon) with a solution of 0.1 *M* TPAP in CH_2Cl_2 which had been stored over molecular sieves No. 5A. Argon was bubbled through the cell followed by electrolysis at 1.5 V to remove oxidizable impurities. Dry porphyrin was then added to reach the desired concentration. Electrolyses required approximately 30 min for completion but were interrupted to record optical spectra. Following oxidation, the solution was reduced at 0.0 V. The number of coulombs transferred during reduction and oxidation agreed within 10%.

Solid $ZnTPP^+ ClO_4^-$ was obtained by oxidation at 0.8 V of ZnTPP in 0.1 *N* TPAP–CH_2Cl_2. CH_2Cl_2 was removed on a rotary evaporator and the residue dissolved in benzene and filtered to remove

(22) M. T. Kelley, H. C. Jones, and D. J. Fisher, *Anal. Chem.*, 31, 956 (1959).

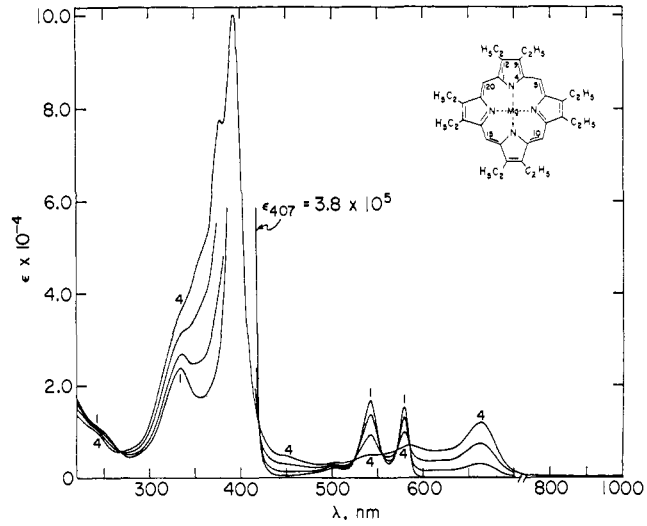

Figure 2. Oxidation of MgOEP in CH_2Cl_2: 1, absorption spectrum of MgOEP; 4, cation radical.

TPAP. The filtrate was taken to dryness and the radical crystallized from CH_2Cl_2. The solid consisted of approximately 90% radical and 10% ZnTPP. Solid $MgOEP^+ ClO_4^-$ was similarly prepared by electrolysis at 0.6 V of MgOEP in CH_2Cl_2.

Chemical Oxidations. Bromine. Aliquots of concentrated solutions of Br_2 in CCl_4 were added to ZnTPP or MgOEP in CH_2Cl_2 under argon and the reactions were followed spectrophotometrically. Oxidation to the radicals required 0.5 mol of Br_2; backtitration with potassium iodide liberated 0.5 mol of I_2. Solid $MgOEP^+ Br^-$ was obtained by oxidation of MgOEP in CH_2Cl_2 followed by removal of the solvent and any excess bromine on a vacuum system. Both the bromide and perchlorate salts of MgOEP are readily reduced by trace impurities.

Xenon Difluoride. XeF_2 was condensed into degassed solutions of ZnTPP in butyronitrile. Oxidation was followed in an optical cell attached to the reaction vessel. Excess XeF_2 oxidized the porphyrin through the dication stage. In solutions saturated with ZnTPP and containing undissolved porphyrin, any dication formed reacted with the excess ZnTPP to yield the radical, and the characteristic spectrum of $ZnTPP^+$ was observed.

Optical and Esr Measurements. Optical absorption measurements were made on a Cary Model 14 spectrophotometer. Low-temperature spectra were obtained in an optical dewar. The temperature was controlled by flowing cold nitrogen through ethanol contained in a copper block and was measured with a thermocouple dipped inside the optical cell.

Time-averaged spectra were obtained with 2047 channel resolution on a Varian 4502 esr spectrometer which was on-line to a computer (SDS Sigma 2). The program developed for simulations of the isototropic hyperfine spectra allowed direct comparison with the experimental data. Radicals were generated by *in situ* electrolysis in a flat quartz cell fitted with a platinum foil electrode and inserted into a gas transfer dewar. Dichloromethane, butyronitrile, or methanol solutions of $\sim 10^{-4}$ *M* porphyrin and 0.1 *M* TPAP were degassed, pressurized with dried argon (~2 atm), and sealed. When these samples were opened and transferred to the electrolysis cell, the escaping argon excluded air from the solution. The radicals were produced by raising the potential until current was observed, and were identified by comparison both with samples transferred from the optical cell and with the solutions prepared *in vacuo* from crystalline radicals. *g* values relative to DPPH were determined in a dual cavity.

Results

Magnesium Octaethylporphyrin. Electrooxidation of magnesium octaethylporphyrin proceeded to completion at 0.6 V *vs.* sce in dichloromethane. (Methanol and butyronitrile were also successfully used as solvents.) Representative absorption spectra, at various stages of oxidation, are displayed in Figure 2. Well-defined isosbestic points testified to the smooth course

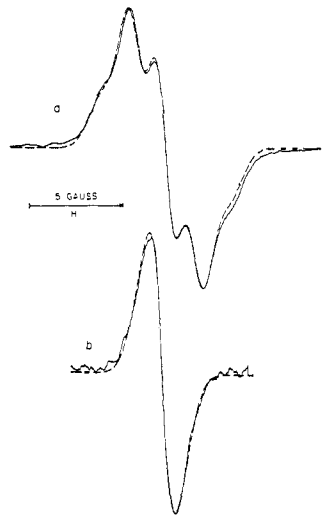

Figure 3. Esr spectra of $MgOEP^+$ (a) and $MgOEP^+$-d_4 (b) in CH_3OH at $-50°$. Dashed lines represent computer simulations: 1.5-G line width, Gaussian line shape, and four equivalent hydrogens, a_H = 1.48 G for a and four equivalent deuteriums, a_D = 0.227 G for b.

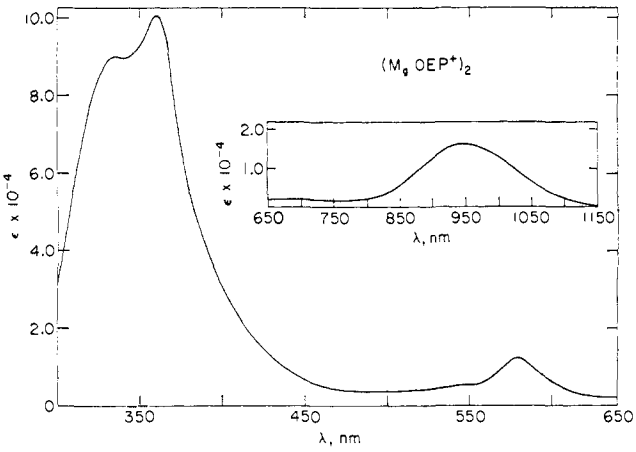

Figure 4. Absorption spectrum of the $MgOEP^+$ dimer in CH_2Cl_2 at $-60°$.

of the reaction. Simultaneous coulometric data obtained during and at the end of the electrolysis indicated that 1.0 (±0.1) electron per molecule was removed. Better than 99% of the initial MgOEP which was oxidized was recovered by electroreduction at 0.0 V or by the use of a mild reducing agent such as potassium iodide.

MgOEP underwent an analogous one-electron oxidation when treated with bromine in either dichloromethane or chloroform. The product was stable in these solvents and spectroscopically resembled the electrolytically generated species. The corresponding salts, $MgOEP^+$ Br^- and $MgOEP^+$ ClO_4^-, were isolated as semicrystalline salts contaminated with MgOEP.

The esr spectrum of the oxidized material in CH_2Cl_2 showed only a single line, 2.5 G wide (peak-to-peak) at g = 2.0025. This signal diminished and finally disappeared as the solution was cooled. Concurrently, the color of the solution changed from blue-green to red. These changes were a function of both solvent and anion. In methanol, the optical spectrum remained unaltered even at $-50°$ but the esr spectrum

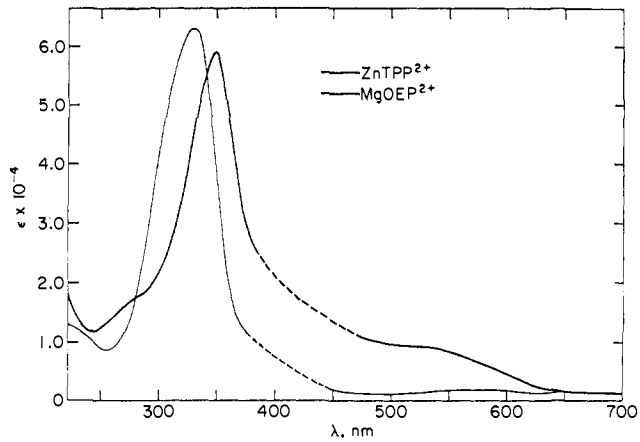

Figure 5. Absorption spectra of dications in CH_2Cl_2: $ZnTPP^{2+}$ (heavy) and $MgOEP^{2+}$ (light). Dotted lines represent region corrected for the Soret bands of trace diacid salts.

of either $MgOEP^+$ Br^- or ClO_4^- partially resolved to five lines,[16b] as shown in Figure 3a. Under similar conditions, oxidized MgOEP-d_4, deuterated at the *meso* positions, exhibited only the narrow singlet shown in Figure 3b. The five lines in the spectrum of $MgOEP^+$ can therefore be assigned to the four hydrogens at the *meso* positions. On the basis of the computer fit shown in Figure 3a, a_H was determined as 1.48 G. On the assumption that deuteration caused no change in spin density, the spectrum of the deuterated species was reconstructed by substituting the nuclear spin of deuterium, I = 1, and a_D = 0.227 G (a_D = 0.1535 a_H because of the magnetic properties of the two isotopes[23]). The simulated and experimental spectra are compared in Figure 3b.

The disparate temperature behavior of $MgOEP^+$ in dichloromethane and in alcohol prompted further study. On cooling, the optical spectrum of $MgOEP^+$ depicted by Figure 2 changed to that shown in Figure 4. This blue-green to red transformation was essentially completed at $-20°$ for $MgOEP^+$ ClO_4^- in CH_2Cl_2 and at $-75°$ in CH_3OH.[24] $MgOEP^+$ Br^- in either CH_2Cl_2 or CH_3OH underwent the color transition near $-70°$. No esr signal at g = 2 or at half-field was found to be associated with the red species either as the bromide or perchlorate salt in CH_3OH or CH_2Cl_2. The initial concentrations and spectra of the cation radical were totally recovered by warming the red solutions to room temperature. The stoichiometry of the reaction was determined from optical data obtained at 0° for $MgOEP^+$ ClO_4 in CH_2Cl_2. At this temperature the radical coexists with the red species. The absorbance at any given wavelength is given by

$$A = \epsilon_1 C_1 l + \epsilon_2 C_2 l$$

where ϵ is the molar extinction coefficient in l./mol cm, C is the concentration in mol/l., and l is the light path in centimeters for the radical (species 1) and the red species (2). Extinction coefficients at 0° were obtained from Figures 2 and 4, respectively, and corrected for volume changes. At 950 nm, $\epsilon_1 \sim 0$, hence $A = \epsilon_2 C_2 l$ and C_2 can be calculated. Since the total concentration of porphyrin is known, C_1 can also be determined.

(23) T. F. Wimett, *Phys. Rev.*, **91**, 499 (1953).

(24) Fuhrhop and Mauzerall[16b] have also observed that $MgOEP^+$ ClO_4^- and $ZnOEP^+$ ClO_4 in CH_3OH absorb in the 950-nm region at low temperatures.

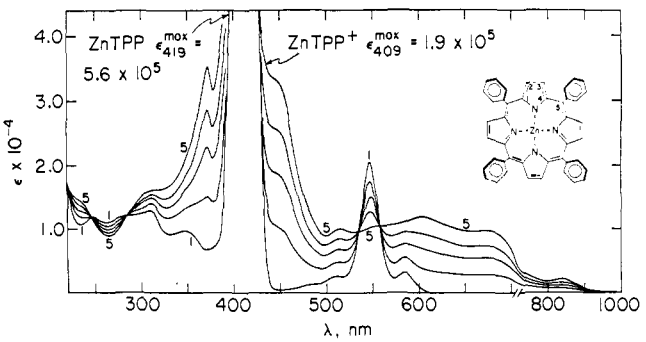

Figure 6. Oxidation of ZnTPP in CH_2Cl_2: 1, absorption spectrum of ZnTPP; 5, cation radical.

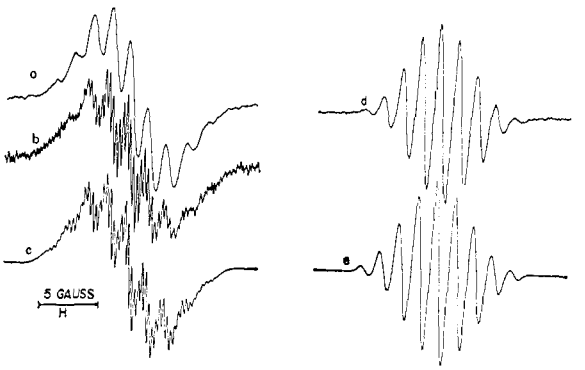

Figure 7. Esr spectra of $ZnTPP^+$ in butyronitrile: (a) characteristic nine lines obtained at room temperature; (b) −54°; (c) computer simulation of b, four equivalent nitrogens, a_N = 1.58 G and eight equivalent hydrogens, a_H = 0.316 G (see text); (d) $ZnTPP^+$-d_{20}, phenyl groups deuterated; (e) computer simulation of d, 0.67-G line width, Gaussian line shape, four nitrogens, a_N = 1.58 G and eight deuteriums, a_D = 0.049 G.

Analysis of data obtained at several wavelengths and over a concentration range of 1–5 × 10^{-4} *M* porphyrin yielded an equilibrium constant of 4.7 (±0.3) × 10^3 l./mol for the formation of a dimer at 0° in CH_2Cl_2

$$2MgOEP^+ \rightleftharpoons (MgOEP^+)_2$$

Other equilibria such as monomer–monomer, monomer–trimer, etc., were not consistent with the experimental results.

Continued electrolysis of $MgOEP^+$ at 0.9 V resulted in a faintly yellow solution characterized by the absorption spectrum[25] shown in Figure 5. Coulometry indicated further loss of 1.1 (±0.1) electron per molecule of radical. No esr signal at $g \sim 2$ was detected for this compound. Two-electron reduction of this new species regenerated >95% of the initial MgOEP. The electroreduction at 0.0 V occurred *via* the cation radical, *viz.*

$$MgOEP^{2+} \xrightarrow{e^-} MgOEP^+ \xrightarrow{e^-} MgOEP$$

The oxidized product also reacted quantitatively with neutral MgOEP according to

$$MgOEP^{2+} + MgOEP \longrightarrow 2MgOEP^+$$

These reactions are clearly consistent with the expected behavior of the dication and rule out the possibility that the oxidized species is a secondary product of the electrode reaction resulting from addition of a nucleophilic impurity to the dication. On the other hand, electrolysis of MgOEP at 0.9 V in CH_2Cl_2 containing 2% of CH_3OH does not yield the absorption spectrum characteristic of the dication.

Zinc Tetraphenylporphyrin. The one-electron oxidation (1.0 ± 0.1 e/molecule) of ZnTPP in CH_2Cl_2 proceeded to completion at 0.8 V with the appearance of several isosbestic points in the optical spectra taken during electrolysis (Figure 6). The final spectrum was independent of temperature from 25 to −80°. The resulting green solution was chemically or electrolytically reduced with recovery of >99% of starting material. Xenon difluoride, bromine, and ceric ammonium nitrate in butyronitrile also afforded the oxidized species. Crystalline $ZnTPP^+$ ClO_4^-, contaminated with a few per cent of parent porphyrin, was isolated from a quantitative one-electron electrolysis.

Esr spectra of the oxidized porphyrin characterized it as a π-cation radical. At room temperature, in dichloromethane, toluene, and methanol–dichloromethane (9:1), $ZnTPP^+$ ClO_4^- exhibited partially resolved spectra with g = 2.0025 and the nine hyperfine lines typified by Figure 7a. Solutions of radicals prepared by *in situ* electrolysis, by dissolving crystalline $ZnTPP^+$ ClO_4^-, or by transferring samples from the optical electrolysis cell all yielded similar spectra. (Oxygen broadened the spectrum and the hyperfine structure was lost. The effect was reversible; removal of oxygen regenerated the original nine lines.)

In butyronitrile additional resolution was obtained at lower temperatures, as shown in Figure 7b. (The smaller splittings were also detected in cold toluene.) The experimental room temperature spectrum was satisfactorily computer simulated by assuming that four equivalent nitrogens with a_N = 1.58 G and eight equivalent hydrogens a_H = 0.316 G give rise to the observed nine-line signal. The spectrum obtained at −50° was also computed by using the same splitting constants. An additional parameter was introduced, however. Two species were presumed present, one which possessed a room-temperature spectrum, *i.e.*, nine lines 1.3 G wide, the other a well-resolved spectrum with line widths of only 0.2 G. The simulated spectrum shown as Figure 7c was obtained by setting the ratio of broad to narrow line spectra at 60:1 and maintaining a_N = 1.58 and a_H = 0.316 G in both. Although the assignments may not be unique, reasonable agreement clearly exists. (Trial values of a_N and a_H were determined directly from the experimental spectra at 25 and −50°, respectively.)

In butyronitrile and at ∼−50°, under conditions where the best resolved spectra of $ZnTPP^+$ were obtained, the cation radical of $ZnTPP$-d_{20} (deuterated phenyl groups) exhibited instead the nine-line spectrum of Figure 7d. The spectrum was simulated (Figure 7e) by retaining four equivalent nitrogens, a_N = 1.58 G, but replacing the eight equivalent hydrogens of a_H = 0.316 G by deuterons with a_D = 0.0486 G.

The deuteration experiment clearly demonstrates that the additional hyperfine structure observed with $ZnTPP^+$ in butyronitrile is due to interaction of the unpaired electron with protons on the *phenyl rings*.

At a potential of 1.1 V electrolysis of $ZnTPP^+$ in dry CH_2Cl_2 resulted in a magenta solution. Coulometric data indicated the abstraction of 1.1 (±0.1) electrons

(25) A small amount (*ca.* 1% of total porphyrin) of the diacid salt of octaethyl porphyrin (H_4OEP^{2+}) is formed, and its Soret band at 403 nm was subtracted from the observed spectrum. The broken line represents the correction.

Table I. Spin Densities in Porphyrin Cation Radicals

Atom	$^2A_{2u}$ state: Spin density, No CI	$^2A_{2u}$ state: Spin density, CI	$^2A_{2u}$ state: a_{exptl} ($ZnTPP^+$), G	$^2A_{2u}$ state: a_{calcd}, G	$^2A_{1u}$ state: Spin density, CI	$^2A_{1u}$ state: a_{exptl} ($MgOEP^+$), G
C-1	0.0066	−0.0094			0.0981	
C-2	0.019	0.0134		0.36[a]	0.0262	
C-5	0.1581	0.1932			0.0012	1.48
N	0.041	0.049	1.58	1.18,[b] 1.55[c]	0.000	
Phenyl H			0.316			

[a] $a_H = 27\rho_H$. [b] $a_N = 24\rho_N$; ref 32. [c] $a_N = 30.9\rho_N - 4\rho_c$; ref 33.

per molecule. The spectrum of the two-electron oxidation product is shown[26] in Figure 5. No esr signal was observed. The following reactions are clearly characteristic of a dication: addition of neutral porphyrin to the product of the two-electron oxidation regenerated the cation radical and electrolytic reduction proceeded *via* $ZnTPP^+$ to ZnTPP. The dication was unstable in the presence of nucleophiles; reaction with water or methanol led to isoporphyrins.[27] Xenon difluoride also oxidized ZnTPP in butyronitrile through the dication stage to yield an isoporphyrin as evidenced by optical spectra. This sets a minimum of 1.1 V (*vs.* sce) for the oxidation potential of XeF_2 in this solvent.

Discussion

This paper establishes the existence of stable π cations of metalloporphyrins. In particular, ZnTPP and MgOEP undergo two successive and reversible one-electron oxidations. The esr results unambiguously demonstrate that the first electron is abstracted from the ligand; unpaired spin is delocalized over the porphyrin ring.

Polarographic data[13] help to establish that the second electron is also removed from the organic moiety. The differences $\Delta = E_{1/2}(2) - E_{1/2}(1)$ between first and second oxidation waves of six metals with the same ligand vary little: PbTPP, 0.33 V; ZnTPP, 0.32 V; MgTPP, 0.32 V; CuTPP, 0.26 V; CdTPP, 0.30 V; and BaTPP, 0.29 V. This constancy is possible only if the dications are formed by ring oxidation. As we will show, agreement between molecular orbital calculations and the observed electronic spectra lends additional support to the π-cation assignments.

The increased resolution of the esr spectra of $MgOEP^+$ in methanol and $ZnTPP^+$ in butyronitrile suggests solvent interactions. Anion radicals are known to exhibit different line widths with varying solvation,[28] and a similar effect involving cation radicals may occur here. In fact, the specific interaction of neutral MgOEP with methanol compared with butyronitrile or dichloromethane is easily demonstrated. Butyronitrile solutions of MgOEP which contain as little as 0.1 *M* methanol exhibit the same optical absorption spectrum as do methanol solutions.

Another demonstration of the importance of solvation is the dimer formation of $MgOEP^+ ClO_4^-$ observed at 0° in CH_2Cl_2 but below −60° in CH_3OH. This solvent and temperature dependence is qualitatively in accord with the expected behavior of triple-ion formation, the theory[29] of which predicts increased association of ions at reduced temperature and in solvents of low dielectric constant. Formulation of the dimer may include, therefore, triple ions consisting of radicals and anions. The disappearance of the esr signal of $MgOEP^+$ with dimerization suggests broadening either due to electronic triplet formation or to creation of a new bond.

SCF-MO Calculations

Electronic Structure of the Cation Radical. Neutral metalloporphyrin spectra have been interpreted with the aid of molecular orbital theory as arising from transitions among four porphyrin π orbitals.[30] The results show that the two lowest pairs of excited configurations ($3a_{2u} \rightarrow 4e_g$, $1a_{1u} \rightarrow 4e_g$) are nearly degenerate, and that the extensive configuration interaction (CI) between them accounts for the high intensity Soret band (B) and low intensity visible bands (Q). A passive role is assigned to the central metal and agreement between general features of calculated and experimental quantities such as absorption spectra and bond lengths is stressed. It is this qualitative picture of the cation radical electronic structure that is our present concern; specifically does a π-electron theory predict reasonable absorption and esr spectra?

The self-consistent field molecular orbital method (SCF-MO) of Pariser, Parr, and Pople can be applied to certain open-shell systems. The theory and its application to a nondegenerate doublet state has been described previously.[31] The semiempirical parameters required in this theory were taken from ref 30, and represent the so-called "standard" set; choice of this set minimizes the theoretical splitting between B and Q bands.

Results of the calculation show that the energetic order of one-electron orbitals is unaltered from that encountered in neutral porphyrin. Thus, the orbital symmetry (D_{4h}) types and energies (in electron volts) of the radical cation are as follows: $2e_g$ (−14.1764), $2a_{2u}$ (−14.0603), $2b_{2u}$ (−14.0255), $3e_g$ (−13.6005), $1a_{1u}$ (−11.9656), $3a_{2u}$ (−10.5997), $4e_g$ (−7.8252); only orbitals pertinent to the subsequent discussion are listed. The ground-state configuration is $(2e_g)^4(2a_{2u})^2(2b_{2u})^2(3e_g)^4(1a_{1u})^2(3a_{2u})^1$ so that the ground electronic state is $^2A_{2u}$. Spin density distributions with and without CI for this state are listed in Table I and show that the spin is localized on the *meso*-carbon atoms.

(26) As was the case with $MgOEP^{2+}$, some diacid salt (H_4TPP^{2+}) is formed; the extent of the side reaction is governed by the dryness of the solvent.

(27) D. Dolphin, R. H. Felton, D. C. Borg, and J. Fajer, *J. Amer. Chem. Soc.*, **92**, 743 (1970).

(28) K. Hofelmann, J. Jagur-Grodzinski, and M. Szwarc, *ibid.*, **91**, 4645 (1969), and references therein.

(29) R. M. Fuoss, *ibid.*, 80, 5059 (1958); **56**, 1857 (1934).

(30) C. Weiss, H. Kobayashi, and M. Gouterman, *J. Mol. Spectrosc.*, **16**, 415 (1965).

(31) J. Fajer, B. H. J. Bielski, and R. H. Felton, *J. Phys. Chem.*, **72**, 1281 (1968).

A variety of equations relating nitrogen splitting constants with spin-density distributions have been proposed. Representative values[32,33] calculated from these are included in Table I. The equations were determined empirically for radicals of six-membered heterocyclic rings and therefore should be applied only semiquantitatively to the nitrogen of a pyrrole ring. Nonetheless, the range of calculated values (1.2–1.6 G) is clearly compatible with assignment of the nine ZnTPP$^+$ hyperfine lines to four equivalent nitrogens rather than to the eight equivalent β protons of the pyrrole rings, since $a_H \sim 0.3$ G is calculated for the latter. We have demonstrated that the hyperfine lines with $a_H = 0.32$ G are associated with phenyl protons. No additional splitting due to β protons was observed.

The following considerations suggest a mechanism by which the phenyl protons can interact with unpaired spin localized on the *meso*-carbon atom. Crystallographic studies have established that the bond between the phenyl group and *meso* carbon varies from 1.50 Å in H_2TPP[34] and ZnTPP[35] to 1.54 Å in MgTPP,[36] while the dihedral angle defined by the planes of the phenyl and porphyrin rings ranges from 60° in ZnTPP[35] to a suggested value approaching 90° in MgTPP.[36] These structural properties rule out extensive conjugation of the phenyl group with the porphyrin. However, the large dihedral angle requires that *ortho* protons project into the π cloud of the porphyrin ring. Then, the McConnell relation becomes invalid since the dominant mechanism of spin delocalization is no longer *via* $\sigma \rightarrow \sigma^*$ excitations, but rather *via* a direct σ–π interaction. This is the view which Pople and Beveridge have employed in their INDO treatment[37] of proton coupling constants in benzyl radical as a function of phenyl ring twist. Coupling constants appropriate to ZnTPP$^+$ can be estimated by combining their results with our calculated value (0.193) of *meso*-carbon spin density. The results, in gauss, as a function of dihedral angle are for *ortho* protons: −0.38 (90°), −0.45 (75°), −0.64 (60°); for *meta* protons: 0.54 (90°), 0.56 (75°), 0.62 (60°); for *para* protons: −0.04 (90°), −0.125 (75°), −0.351 (60°). The large values for *meta* protons are an artifact of the INDO calculation.[36] Further, the assumed bond length in the INDO calculation was 1.40 Å, and the longer 1.50-Å distance in ZnTPP will act to diminish predicted coupling constants. These results are thus compatible with the observed splitting constant $a_H = 0.32$ G of the phenyl protons. Without selective deuterium labeling, we cannot specify which of these protons causes the observed hyperfine structure.

Energies of optically accessible, singly excited states (^2E_g) are displayed in Figure 8 prior to and after CI, with parentage of the interacted states indicated. The experimental values obtained from maxima of Figure 6 are compared with the calculated spectrum; tentative assignments are indicated. The intense band at 24,450

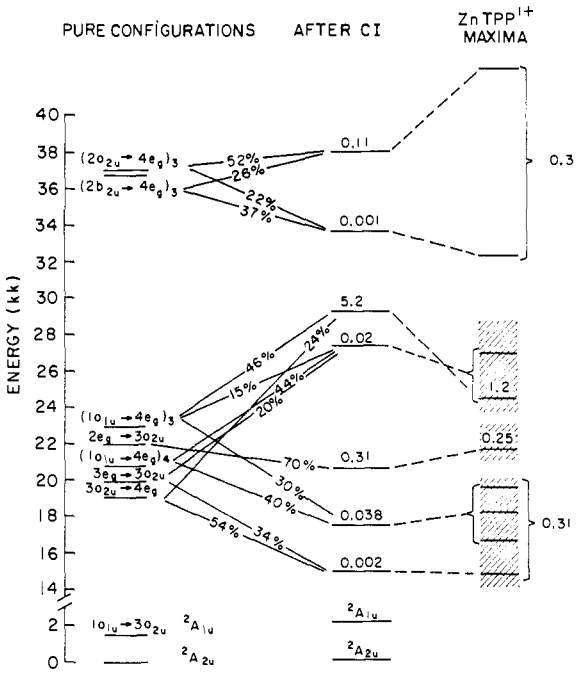

Figure 8. State energies of a porphyrin cation radical. Numbers in last two columns are, respectively, theoretical and experimental oscillator strengths. Subscripts on pure configurations refer to spin functions: $\chi_3 = 2^{-1/2}(\alpha\alpha\beta - \beta\alpha\alpha)$ and $\chi_4 = 6^{-1/2}(2\alpha\beta\alpha - \alpha\alpha\beta - \beta\alpha\alpha)$. Percentages refer to amount of pure configuration in state after CI. Shaded areas indicate spread of experimental absorption bands. Optically accessible states are ^2E_g.

cm^{-1} (409 nm) arises from those transitions responsible for the Soret band of neutral metalloporphyrins. In the radical only three electrons may be promoted rather than the four electrons available in the neutral porphyrin. This simple model thus predicts a cation Soret band only $^3/_4$ as intense as the porphyrin Soret band; the SCF–MO calculations predict a ratio of 0.7. The experimental value[38] is 0.6 ± 0.1.

Evidence exists to strengthen the theoretical prediction that the visible spectrum (430–700 nm) consists of several electronic transitions. Replacement of an *ortho*-phenyl hydrogen by a fluorine atom is expected to perturb most strongly those molecular orbitals which have a large MO coefficient at the *meso* carbon. Examination of Figure 8 reveals that the calculated transitions at 14,750 cm^{-1} and 20,630 cm^{-1} contain, respectively, 88 and 70% of configurations involving excitation to or from the a_{2u} orbital. It is just this orbital which should be affected by the fluorine substitution. In the esr spectrum of the cation radical[39] of zinc *meso*-tetra(*o*-fluorophenyl)porphyrin, $a_N = 1.2$ G compared with 1.6 G in ZnTPP$^+$; the optical spectrum displays intensity changes at 14,600 cm^{-1} (685 nm) and 21,740 cm^{-1} (460 nm) while the other maxima are unaltered.

The major conclusion reached from the above discussion is that ZnTPP$^+$ displays physical properties consonant with a $^2A_{2u}$ ground electronic state. If the same theoretical description were valid for MgOEP$^+$, then a_H for protons attached to *meso*-carbon atoms should be *ca.* 4–5 G. Instead we find $a_H = 1.48$ G,

(32) P. Smejtek (*Collect. Czech. Chem. Commun.*, 31, 260 (1966)) derived a McConnell equation from radical-cation data.
(33) E. G. Janzen and J. W. Happ (*J. Phys. Chem.*, 73, 2335 (1969)) derived a McConnell equation from radical-anion data.
(34) S. J. Silversand and A. Tulinsky, *J. Amer. Chem. Soc.*, 89, 3331 (1967).
(35) M. D. Glick, G. H. Cohen, and J. L. Hoard, *ibid.*, 89, 1996 (1967).
(36) R. Timkovich and A. Tulinsky, *ibid.*, 91, 4430 (1969).
(37) J. A. Pople and D. L. Beveridge, *J. Chem. Phys.*, 49, 4725 (1968).
(38) The oscillator strength of the ZnTPP Soret band was found to be 1.9.
(39) Unpublished results.

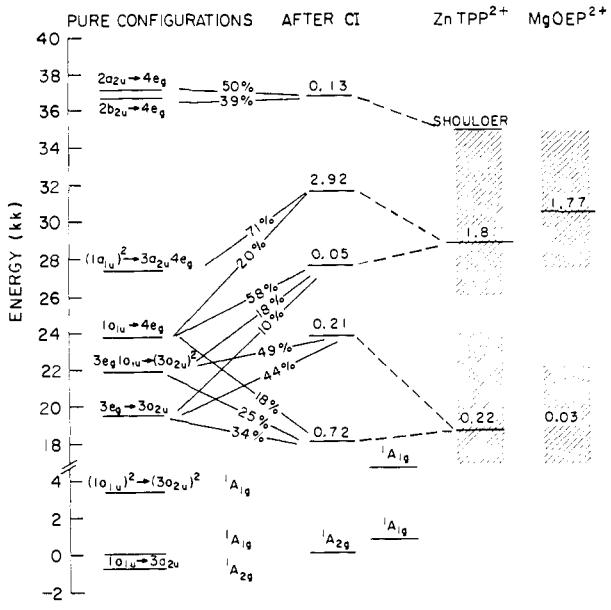

Figure 9. State energies of porphyrin dications. Numbers in column labeled "after CI" are theoretical dipole oscillator strengths. Numbers in last two columns are experimental oscillator strengths. Optically accessible states are ^1E_u.

and no nitrogen hyperfine lines are resolved.[40] To account for this change, we suggest that MgOEP$^+$ is characterized by a $^2A_{1u}$ ground electronic state in which a hole is now present in the $1a_{1u}$ orbital. A distinguishing feature of this state will be little spin density at *meso*-carbon atoms and nitrogen atoms.

The energy separation of the $^2A_{1u}$ and $^2A_{2u}$ states must be small in order that the possible interactions which select one or the other state be operative. The energy difference can be estimated from the SCF–MO calculations and it ranges between 1450 and 2050 cm^{-1} (see Figure 8). Such differences are sensitive to slight alterations in SCF–MO semiempirical parameters. If, for example, α_c for the *meso* carbon is changed from -11.22 eV to -11.90 eV, we find the $^2A_{1u}$ state is *more stable* than the $^2A_{2u}$ state by 2000 cm^{-1} before CI and 1140 cm^{-1} following CI. The spin-density distributions are impressively changed: $\rho_N = 0.0000$ and ρ_c (*meso*) $= 0.0012$; spin densities localized on the remaining atoms are given in Table I. The calculation cited here clearly does not yield the 1.5-G splitting observed for MgOEP$^+$ and is only meant to be indicative.

Doubly excited configurations are necessary for a proper theoretical treatment of the MgOEP$^+$ absorption spectrum. It is clear that the ^2E_g state obtained from $(1a_{1u})^2 \rightarrow 3a_{2u}4e_g$ is singly excited with respect to $1a_{1u} \rightarrow 3a_{2u}$ and will be optically allowed. Preliminary computations which include some doubly excited states of $^2A_{1u}$, $^2A_{2u}$, and ^2E_g symmetry have demonstrated that the optical spectrum of a porphyrin cation radical whose ground state is $^2A_{1u}$ will be qualitatively similar to that of the $^2A_{2u}$ ground state; there are several transitions of moderate intensity between 500 and 690 nm and a strong transition in the ultraviolet.

Electronic Structure of the Dication. Both ZnTPP^{2+} and MgOEP^{2+} possess similar optical spectra: strong absorption to the blue of the neutral or cation-radical Soret bands and weaker, unstructured absorption in the visible spectrum (Figure 5). A closed-shell SCF–MO calculation using the previous semiempirical parameters and including doubly excited states gave the results exhibited in Figure 9. Tentative assignments of the experimental spectra are shown as well as principal contributing configurations. It is important to note that the ground state of the dication after CI is found to be a $^1A_{2g}$ state arising from the configuration $(2e_g)^4(2a_{2u})^2(2b_{2u})^2(3e_g)^4(1a_{1u})^1(3a_{2u})^1$ and is not the $^1A_{1g}$ state that consideration of one-electron energies would have predicted. This calculation also demonstrates the necessity of including doubly excited states for a proper interpretation of the optical spectrum, since the intense band at 31,440 cm^{-1} arises from such a configuration. The experimental ratio of oscillator strength of the intense bands found in the dication to that of the neutral porphyrin Soret band is 0.95 ± 0.15. A theoretical value of 0.91 for this ratio is determined from the calculated oscillator strength of the dication (Figure 9) and the oscillator strength computed for neutral porphyrin with doubly excited states included.[41]

The $^1A_{1g}$ state lies only $\sim$800 cm^{-1} above the $^1A_{2g}$ state. The interactions which determine the ground state of the cation radical also operate for the dication. The optical data alone are not sufficient to exclude categorically a $^1A_{1g}$ dication ground state.

These computations demonstrate some effects of the near degenerate states formed from $3a_{2u}$ and $1a_{1u}$ orbitals. Lhoste, Helene, and Ptak[42] similarly explained the differing zero-field splitting constants of porphyrin triplets obtained by photolysis. They, and earlier Gouterman,[43] pointed out that two nearly degenerate ^3E_u states are formed by the excitations $1a_{1u} \rightarrow 4e_g$ and $3a_{2u} \rightarrow 4e_g$ and suggested that both triplet states were detected.

Concluding Remarks

We have stressed the sequential oxidations of the ligands in ZnTPP and MgOEP. This sequence is not unique; we will shortly present optical and esr evidence[1] which confirms that MgTPP, ZnOEP, CuTPP, CuOEP, CdTPP, and zinc etioporphyrin I behave similarly when electrooxidized. However, when metals capable of more than one oxidation state are incorporated into the porphyrin, metal oxidation may occur.[1,17,18] For example, Co(II)TPP and Co(II)OEP are initially oxidized to the corresponding cobaltic species followed by ligand oxidation at higher potentials. In these cases, spin density is transferred from the oxidized rings onto the metal: $a_{Co} = 5.7$ G and 1.4 G for Co(III)TPP^{2+} and Co(III)OEP^{2+}, respectively. Fe(II)OEP yields Fe(III)OEP$^+$ and then a new species which, on the basis of polarographic and optical data, is also formulated as a ring oxidation product.

The properties discussed here are relevant to those porphyrins and related compounds which function in biological systems. An increasing body of data suggests that primary photosynthetic processes involve

(40) The MgOEP$^+$ spectra of Figure 3 can also be simulated by assuming that $a_N \leq 0.3$ G, $a_H = 1.48$ G, and by narrowing the line width.

(41) Inclusion of doubly excited states in neutral porphyrin calculations reduces the Soret oscillator strength from 6.7 to 3.22.

(42) J. M. Lhoste, C. Helene, and M. Ptak in "The Triplet State," A. B. Zahlan, Ed., University Press, Cambridge, Mass., 1967, p 479.

(43) M. Gouterman, *J. Chem. Phys.*, 33, 1523 (1960).

oxidation of chlorophyll[5,6] and bacteriochlorophyll.[44] Considering MgTPP or MgOEP as model systems, we suggest that the oxidized chlorophylls are properly characterized as π-cation radicals. Indeed, electrooxidation[1] of ethyl chlorophyllide a and chlorophyll a converts these molecules into bleached species whose optical and esr properties are consistent with this identification. An additional feature of the magnesium porphyrins is that these molecules are easily oxidized, a fact which may account for the appearance of magnesium chlorins in the photosynthetic apparatus. In the instance of catalase and peroxidase function, the oxidation of the prosthetic heme group is usually formulated as metal oxidation[4] to yield Fe(IV) and Fe(V). An alternative, tentatively supported by our results, suggests that ring oxidation as well as metal oxidation should be considered.

(44) J. D. McElroy, G. Feher, and D. C. Mauzerall, *Biochim. Biophys. Acta*, 172, 180 (1969); J. R. Bolton, R. K. Clayton, and D. W. Reed, *Photochem. Photobiol.*, **9**, 209 (1969).

Acknowledgments. We wish to thank Professor D. Mauzerall for discussions on the nature of the oxidation products and D. van der Kolk for technical assistance. This work was supported in part by the U. S. Atomic Energy Commission, in part by the Petroleum Research Fund of the American Chemical Society (PRF-849-G1), and in part by the Research Corporation.

Deuterium Isotope Effects on the Fluorescence of Tryptophan in Peptides and in Lysozyme[1]

Sherwin S. Lehrer

Contribution from the Department of Muscle Research, Retina Foundation, Institute of Biological and Medical Sciences, and the Department of Neuropathology, Harvard Medical School, Boston, Massachusetts 02114.
Received October 31, 1969

Abstract: A study has been made of the variation of fluorescence with pH and pD for the tryptophan model compounds, skatole, L-trp, L-trp-L-tyr, and N-Cbz-L-trp-L-tyr, and for the tryptophyl fluorescence of lysozyme and of the lysozyme–triNAG complex. Shifts of the fluorescence transitions by 0.3–0.7 pH unit in D_2O compared to H_2O gave further evidence for the involvement of amino, carboxyl, and phenol groups in the quenching of tryptophyl fluorescence. The large isotope effects observed are consistent with the expected decreased rate of deuteron transfer when the protons of the amino and carboxyl groups are exchanged for deuterons in D_2O. The value for the ratio of the rate constant for the intramolecular quenching by the NH_3^+ group of L-trp in H_2O and D_2O was calculated to be 2.7 from the experimental data and a simple kinetic scheme. A large isotope effect was also observed for the intermolecular quenching of indole-3-acetamide by glycine at neutral pH. These data are consistent with a proton transfer quenching mechanism. The results of the study with lysozyme provide further evidence for the involvement of acid groups in the quenching of tryptophan fluorescence.

A number of recent studies have dealt with deuterium isotope effects on the fluorescence of indole and tryptophan compounds.[2-4] Stryer, for example, showed that for a variety of fluorophors with exchangeable protons the slower rates of deuteron transfer *from the fluorophor* to the solvent adequately explained the isotope effect.[2] The possibility appears, however, that deuterium isotope effects can also be caused by the decreased rate of proton transfer from a quencher *to the fluorophor*. This will be especially important for those systems in which the protonated form of the excited fluorophor has reduced fluorescence, as appears to be the case for indole compounds.[5] In particular, intramolecular proton transfer from the amino and carboxyl groups to the indole ring of L-trp[6] and tryptophyl dipeptides has been suggested as a quenching mechanism.[7] In view of the slower transfer rate of the deuteron, fluorescence differences are to be expected in these systems. In proteins such effects may be observable if a proton donating group is located near an indole side chain. This study of tryptophyl fluorescence as a function of pH in H_2O and D_2O provides further evidence that a major contribution to the deuterium isotope effect observed in such compounds is due to proton transfer to the fluorophor.

Experimental Section

Highly purified samples of L-trp (Mann Research, N. Y.), L-trp-L-tyr (Cyclo Chemical Corp., Los Angeles, Calif.), and N-Cbz-L-trp-L-tyr (Cyclo) were used without further purification. Lysozyme was obtained from Worthington Biochemical Corp., Freehold, N. J., and triNAG was obtained through the courtesy of Dr. J. Rupley. Indole (Fisher Scientific, Boston) and skatole

(1) Presented at the Symposium on Biological Molecules and their Excited States, Arden House, New York, N. Y., Oct 1969. This work was supported by grants from the National Institute of Arthritis and Metabolic Diseases, National Institutes of Health (5-RO1 AM 11677), and the Massachusetts Heart Association (#816).
(2) L. Stryer, *J. Amer. Chem. Soc.*, 88, 5708 (1966).
(3) M. S. Walker, T. W. Bednar, and R. Lumry in "Molecular Luminescence," E. C. Lim, Ed., W. A. Benjamin, Inc., New York, N. Y., 1969, p 135.
(4) J. Eisinger and G. Navon, *J. Chem. Phys.*, 50, 2069 (1969).
(5) J. W. Bridges and R. T. Williams, *Biochem. J.*, **107**, 225 (1968).
(6) The following abbreviations are used: L-trp = L-tryptophan; L-tyr = L-tyrosine; N-Cbz = N-carbobenzoxy; triNAG = tri-N-acetyl-D-glucosamine.
(7) G. Weber in "Light and Life," W. McElroy and B. Glass, Ed., Johns Hopkins University Press, Baltimore, Md., 1961, p 82.